AIP | Journal of Applied Physics

Anisotropy of strain relaxation in (100) and (110) Si/SiGe heterostructures

H. Trinkaus, D. Buca, R. A. Minamisawa, B. Holländer, M. Luysberg et al.

Citation: J. Appl. Phys. **111**, 014904 (2012); doi: 10.1063/1.3672447
View online: http://dx.doi.org/10.1063/1.3672447
View Table of Contents: http://jap.aip.org/resource/1/JAPIAU/v111/i1
Published by the American Institute of Physics.

Additional information on J. Appl. Phys.

Journal Homepage: http://jap.aip.org/
Journal Information: http://jap.aip.org/about/about_the_journal
Top downloads: http://jap.aip.org/features/most_downloaded
Information for Authors: http://jap.aip.org/authors

ADVERTISEMENT

Downloaded 15 May 2013 to 134.94.122.141. This article is copyrighted as indicated in the abstract. Reuse of AIP content is subject to the terms at: http://jap.aip.org/about/rights_and_permissions

Anisotropy of strain relaxation in (100) and (110) Si/SiGe heterostructures

H. Trinkaus,[1] D. Buca,[1,a)] R. A. Minamisawa,[1] B. Holländer,[1] M. Luysberg,[2] and S. Mantl[1]
[1]*Peter Grünberg Institute 9 (PGI 9 -IT) and JARA-FIT, Forschungszentrum Jülich GmbH, D-52425 Jülich, Germany*
[2]*Peter Grünberg Institute 5 (PGI 5) and ER-C Ernst Ruska Center, Forschungszentrum Jülich GmbH, D-52425 Jülich, Germany*

(Received 1 July 2011; accepted 22 November 2011; published online 5 January 2012)

Plastic strain relaxation of SiGe layers of different crystal orientations is analytically analyzed and compared with experimental results. First, strain relaxation induced by ion implantation and annealing, considering dislocation loop punching and loop interactions with interfaces/surfaces is discussed. A flexible curved dislocation model is used to determine the relation of critical layer thickness with strain/stress. Specific critical conditions to be fulfilled, at both the start and end of the relaxation, are discussed by introducing a quality parameter for efficient strain relaxation, defined as the ratio of real to ideal critical thickness versus strain/stress. The anisotropy of the resolved shear stress is discussed for (001) and (011) crystal orientations in comparison with the experimentally observed anisotropy of strain relaxation for Si/SiGe heterostructures. © *2012 American Institute of Physics*. [doi:10.1063/1.3672447]

I. INTRODUCTION

Solid systems far from equilibrium play a key role in modern material science. A special class of such systems is formed by solids implanted with gas atoms of low solubility, particularly with inert gas atoms, which strongly tend to precipitate into bubbles. The broad interest in this class of systems started from their wide application ranging from low-activation structural material for fusion reactors to innovative substrate engineering, like silicon-on-insulator (SOI) or strained Si materials for state of the art MOSFET devices.

The acceptance of strained Si as one of the most promising channel materials for improved CMOS performance triggered the development of virtual SiGe substrate fabrication.[1] Several methods use ion implantation as a mean to generate strain relaxation of SiGe layers.[2–6] As different strain types (tensile, compressive, biaxial, or uniaxial) modify in a specific way the material properties, i.e., carrier mobility,[7,8] dopant diffusion,[9] or dopant solubility,[10,11] the study of dislocation formation and control in Si(Ge) materials regained importance.

In this paper, we explain analytically the experimental observations regarding the relaxation of pseudomorphically grown SiGe layers on (100) and (110) Si substrates using ion implantation and annealing. The work was motivated by the recent experiments on strain relaxation of SiGe(011) layers, which afar from providing a pure (not asymmetric) uniaxial relaxation, indicated strong strain relaxation while the same layer configuration on (001) orientation remained pseudomorphic.[12] The paper reviews the physics of the various relaxation process stages, starting with the He platelet formation to the threading dislocation dynamics, with emphasis on the role of surface orientation. Particularly, the anisotropic critical conditions for layer relaxation are discussed in terms of layer symmetry in an appropriate dislocation model. In addition, a quality parameter for efficient strain relaxation is introduced to establish a basis for comparing theoretical and experimental results.

For the purpose of clarity, the strain/stress relaxation by ion implantation and annealing starts with the generation of dislocation loops, i.e., from over-pressurized He filled cavities in the Si substrate for He implantation[3] or from {311} defects for Si ion implantation.[6] During annealing, these loops glide toward the Si/SiGe interface and then further to the surface, accompanied by the extension of the formed threading dislocations (TDs) through the SiGe layer. It results in the formation of a strain relaxing network of misfit dislocations (MDs) at the SiGe/Si interface.[3,5] The validity of this analytical model proposed by Trinkaus *et al.*[3] in 2000 was later on proven experimentally by *in situ* transmission electron microscopy by Hueging *et al.*[13] and by computer simulations by Schwarz.[14]

II. PLATELETS, DISLOCATION LOOPS AND THEIR INTERACTIONS WITH INTERFACES/SURFACES

A. Platelet formation - crystallographic plane preference

Bubble formation in solids generally requires both gas and matrix atom diffusion. In a crystalline matrix, light gas atoms such as H and He commonly diffuse as interstitial atoms. At medium temperatures, interstitial gas atoms are already mobile while matrix atoms are still immobile. A process, for which no matrix atom transport is required, is the precipitation of the mobile gas atoms between atomic layers of the matrix lattice thus forming gas-filled Griffith cracks.[15] The formation of clusters of helium atoms and vacancies He_mV_n has been discussed in several previous studies[16,17] and supported by the experimental finding of plate shaped precipitates, in fair agreement with previous analyses

a)Electronic mail: d.m.buca@fz-juelich.de.

 © 2012 American Institute of Physics

Downloaded 15 May 2013 to 134.94.122.141. This article is copyrighted as indicated in the abstract. Reuse of AIP content is subject to the terms at: http://jap.aip.org/about/rights_and_permissions

demonstrating the existence of crack like precipitates in silicon.[18]

Here we discuss the preferential formation of platelets, in the face-centered cubic (FCC) system and in particular for Si(Ge). Due to the anisotropy of the silicon lattice the agglomeration process will occur differently for various $\{hkl\}$ planes. For a system taking only discrete values of energy, the probability distribution of platelet planes, or the probability of formation on a $\{hkl\}$ plane, P_{hkl}, is characterized by the probability of finding the system in a particular microscopic state hkl with energy level $(F_{pl})_{hkl}$. The corresponding frequency distribution can be calculated through the canonical partition function Z:[19]

$$P_{hkl} = g_{hkl} e^{-F_{pl}/2} 1/Z, \quad \text{with} \quad Z = \sum_{hkl} g_{hkl} e^{-(F_{pl})_{hkl}/2}, \quad (1)$$

where g_{hkl} is the degeneracy factor, or in our case, the number of equivalent configurations (meaning {hkl} planes) and is given in Table I. In the "Griffith crack" approximation the free energy F_{pl} is given by[16]

$$F_{pl} = 2\pi\gamma r^2 + \frac{\pi^2}{6} r u^2 \frac{E}{1-\nu^2} + F_{gas}(V); \quad V = \frac{4}{3}\pi r^2 u, \quad (2)$$

where r is the platelets radius, u is the elastic (crack) opening displacement, γ is the specific surface (interface) energy, E is the Young's modulus, ν is Poisson's ratio, and F_{gas} is the free gas energy. By replacing the pressure p and the displacement u for a crack in equilibrium, determined from the minimization of the free energy with respect to u and r (i.e., $\partial F_{pl}/\partial u = 0$, $\partial F_{pl}/\partial r = 0$, and $p = -\partial F_{gas}/\partial V$), results in

$$F_{pl} = \frac{5}{4}\left\{\frac{2\pi^3}{3} V^4 \gamma^3 \left(\frac{E}{1-\nu^2}\right)^2\right\}^{1/5} + F_{gas}(V). \quad (3)$$

In an anisotropic crystal such as Si, the appropriate anisotropic extension has to be used: the anisotropic specific surface (interface) free energy γ_{hkl} is that of the habit plane $\{hkl\}$ and the appropriate anisotropic extension of $E \rightarrow (S_{ll,hkl})^{-1}$, where $S_{ll,hkl}$ is the longitudinal elastic modulus in $\langle hkl \rangle$ direction

$$F_{pl} = f(V/\Omega)^{1/5} + F_{gas}(V) \text{ with } = 2.25\left\{\left[\Omega^4 \gamma_{hkl}^3 / S_{ll,hkl}^2\right]\right\}^{1/5}, \quad (4)$$

where $\Omega = 2 \times 10^{-2}$ nm^3 is the atomic volume.

TABLE I. The numerical value of F_{pl} (kT_m), γ_{hkl}, S_{hkl}, g_{hkl}, and the corresponding frequency distribution of platelets, P_{hkl}, for the main crystallographic planes and directions.

$\{hkl\}$	100	110	111	113
γ_{hkl} (J/m^2)	1.36	1.43	1.23	1.38
S_{hkl} (10^{-12} Pa^{-1})	**7.68**	5.92	5.33	6.57
F_{pl} (kT_m)	**37.0**	42.3	40.3	39.7
g_{hkl}	6	12	8	24
P_{hkl} (%)	**98.3**	0.005	0.16	1.6

Energetically, platelets should favor habit planes $\{hkl\}$ where γ_{hkl} is as small as possible. However, the value of f is dominated by the elastically softest $\langle hkl \rangle$ direction, meaning maximum S_{hkl}. The value of f (in units of thermal energy at melting point, kT_m) calculated using specific surface (interface) free energy γ_{hkl} according to Eaglesham *et al.*,[20] and the corresponding frequency distribution of platelets, P_{hkl}, for $T = T_m/2$ are listed in Table I for the main crystallographic planes and directions.

According to Table I, *the energetically most favorable habit planes for platelet formation*, even for the smallest platelet volume, $V = \Omega$, *are the {100} planes.*

B. Interactions with interfaces/surfaces

Once formed, the platelets conserve their metastable configuration as long as any form of matrix diffusion is negligible. During annealing, the low temperature configurations transform, under partial pressure relaxation, into energetically more favorable complexes consisting now of three-dimensional (spherical) bubbles and dislocation loops of self-interstitial type. The assumed restriction of matrix atom transport to internal surfaces and dislocation cores is confirmed by the experimental observation that the total volumes of atoms of the bubble and the loop components are equal in such complexes.[17,21]

Volume increase and pressure relaxation of the gas filled platelets by punching off loops, for a highly degenerated structure of cubic Si, occurs in only 8 of the 12 $\langle 110 \rangle$-loop configurations while for 4 loop configurations the force acting on them is zero. The 8 possible loops configurations surrounding a (001) platelet are schematically displayed in Fig. 1, where the loops (dashed lines) and their Burgers vectors are indicated. For an infinite Si crystal, all possible $\{001\}$ platelets with their 8 corresponding loop configurations are expected to form with equal probability. However, in the case that the platelets are formed close to a surface or

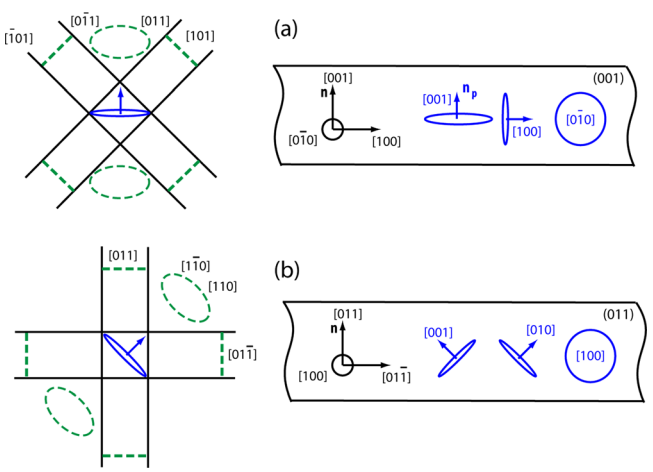

FIG. 1. (Color online) (a) For a platelet with a (001) habit plane (full lines), the eight possible dislocation loop configurations are indicated by dash lines. The (001) platelet is seen along the $[0\bar{1}0]$ direction. On the right hand side, the three possible platelet configurations are sketched for a (001) surface. (b) Orientation of platelets and loops below a (011) system.

Downloaded 15 May 2013 to 134.94.122.141. This article is copyrighted as indicated in the abstract. Reuse of AIP content is subject to the terms at: http://jap.aip.org/about/rights_and_permissions

TABLE II. Summary for configurations of platelets and loops below a (001) and a (011) surface. The strength of the interaction between platelet and surface is given by the angle between platelet normal $\vec{n}_p$ and surface normal $\vec{n}$. The interaction of a dislocation with the surface is determined by the angle between Burgers vector $\vec{b}$ and surface normal $\vec{n}$. Since the interaction of platelets or loops with the surface (or interface) depends strongly on the distance, the strength of the interaction is only indicated qualitatively.

Layers	**(001)**			**(011)**		
Platelets	(001)	(100)	(010)	(010)	(001)	(100)
$\sphericalangle(\vec{n}_p, \vec{n})$	**0°**	90°	90°	**45°**	**45°**	90°
Interaction platelets - layer/surface	**maximum**	minimum	minimum	**medium**	**medium**	minimum
Active BVs	[101], [10$\bar{1}$][011], [01$\bar{1}$]	[101] [10$\bar{1}$]	[011] [01$\bar{1}$]	[110] [1$\bar{1}$0]	[101] [10$\bar{1}$]	[110], [1$\bar{1}$0] [101] [10$\bar{1}$]
$\sphericalangle(\vec{b}, \vec{n})$	**45°**	45°	45°	**60°**	**60°**	60°
Interaction loops -layer/surface	**medium**			weak		
Inactive BVs	–	[110], [1$\bar{1}$0]		[011][a], [01$\bar{1}$]		–

[a]For a platelet under surface the interaction is maximum but the BV is inactive for SiGe strain relaxation.

an interface this equal distribution of configurations does not hold. Instead, the interaction of the stresses arising from the over-pressurized platelets with the free surface is largest for platelets being parallel to the surface. Hence, below a surface with normal $\vec{n} = [\mathbf{001}]$ platelets with a (001) habit plane form predominantly and below a (011) surface with normal $\vec{n} = [\mathbf{011}]$ platelets being inclined by 45° are favored, i.e., with a (010) or (001) habit plane. This analytical considerations on platelet formation are demonstrated by the experiments of Fichtner *et al.*[16] and Hueging *et al.*,[11] which observed that nearly all the platelets nucleate with a surface normal to the {100} plane of the Si matrix. Moreover, 66% of the platelets in a (001) Si crystal were oriented parallel to the surface while the (010) and (100) orientations were found with the occurrence of only 19% and 15%, respectively.[22]

Now, let us consider a (strained) SiGe layer and platelets formed below the interface within the Si substrate. Since the platelets, which are introduced below the SiGe layer, act as internal dislocation sources, an efficient relaxation of the SiGe layer can be achieved.[3,23] All possible platelet and loop configurations which contribute to the relaxation of a SiGe layer are summarized in Table II. In the first rows the different types of platelets and their interaction strength with the surface (interface) are given. Since the interaction strongly depends on the distance of the platelets to the interface, the interaction strength is only indicated by qualitative measures. Nonetheless, platelets with maximum interaction strength will be favored. Two contributions will affect the motion of the dislocation loops generated by the platelets: (i) the free surface and (ii) the stress imposed by the biaxially strained layer. The latter one will only attract dislocation segments, which relax the strain. For the (001) case, these are dislocations having Burgers vector component [100] or [010], which holds for all Burgers vectors listed as "active" in Table II. For the case of a (011) surface, the Burgers vector [011] is the most efficient one to relax the strain surrounding the platelet. However, this Burgers vector will be inactive, since it does not contribute to any strain relaxation of the SiGe layer, as will be demonstrated in the next section. Hence, only Burgers vectors being inclined by 60° contribute to the relaxation process of both, the platelets and the SiGe layer. For layer relaxation, the following conditions have to be fulfilled:

- Platelet configurations with highest efficiency should be favored and configurations with low efficiency must be suppressed;
- Loops should be efficiently attracted to interface and surface.

From the Table II, the following conclusion can be drawn:

(i) *The efficiencies of platelets as dislocation sources are equal for (001) and (011)*;
(ii) **(001)**: *The most favorable platelet* configurations produce the *most active loops*;
(iii) **(011)**: *Least favorable platelet* configurations produce the *most active loops*. Moreover, the *loops are less attracted* to interface and surface.

Possible improvements of the efficiency for strain relaxation can be: ion implantation closer to interface, thinner SiGe-layer or platelet localization on a defined habit plane. The preferential nucleation of He platelets in the Si substrate can be realized by the introduction (epitaxial growth) of an "impurity" layer which either reduces the energy associated with cavity formation, e.g., a SiGe layer[24,25] or by creating additional volume for He accumulation through introduction of smaller substitutional atoms, e.g., Si:C layer.[26,27] Such structures localize and homogenize the planar distribution of the dislocation loop sources (platelets) sensibly increasing the SiGe degree of relaxation.[27]

III. ANISOTROPY OF CRITICAL CONDITION FOR LAYER RELAXATION

As stated above, the fundamental mechanism of layer relaxation is based on stress driven glide of two TDs in opposite directions along an appropriate glide plane, extending by this the strain/stress relaxing MD segment connecting the two TDs arms.[28] The dependence of the force on the dislocation in the glide plane and the line tension of the dislocation will be discussed next. The film thickness above which strain relaxation occurs and the kinetics of the process will be derived by considering the energies associated with a dislocation and the elastic strain, or equivalently, the forces that act on the dislocation.

The driving force for relaxation is due to the misfit strain, $\boldsymbol{F}_{\sigma}$, while the main opposing force is the line tension

Downloaded 15 May 2013 to 134.94.122.141. This article is copyrighted as indicated in the abstract. Reuse of AIP content is subject to the terms at: http://jap.aip.org/about/rights_and_permissions

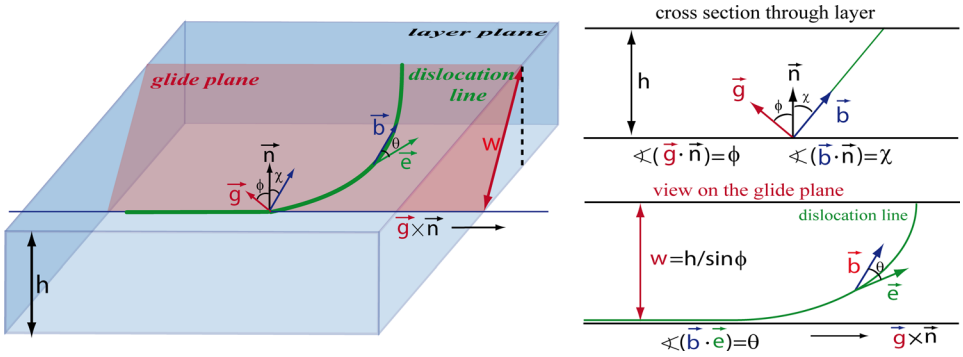

FIG. 2. (Color online) Schematic illustration of a treading dislocation in a crystal. The main vectors are $\vec{n}$: layer normal vector; $\vec{g}$: glide plane normal vector; $\vec{b}$: Burgers vector, $\vec{e}$: unit vector along dislocation line.

of the dislocation, $\boldsymbol{T}$, (and in case of partial dislocations neglected here, the stacking fault energy). Other forces opposing to the relaxation such as frictional forces are negligible at the annealing temperatures used in the relaxation experiments. Figure 2 illustrates schematic the main vectors relevant for the analytical description of forces acting on strain relaxing dislocations in a lattice mismatched system.

In a strained crystalline material, the stress induced force per unit length of a dislocation of Burgers vector $\vec{b}$ is given by the Peach-Koehler formula[29]

$$\boldsymbol{F}_{\sigma} = \left(\bar{\sigma}\cdot\vec{b}\right)\times\vec{l}. \tag{5}$$

For the force along the glide plane, $\boldsymbol{F}_{\sigma}$, only the shear component of the stress tensor $\bar{\sigma}$ is relevant

$$\boldsymbol{F}_{\sigma} = \left(\vec{g}\cdot\bar{\sigma}\cdot\vec{b}\right)\left(\vec{g}\times\vec{l}\right), \tag{6}$$

where $\vec{g}$ is the normal vector to the glide plane, $\left(\vec{g}\cdot\bar{\sigma}\cdot\vec{b}\right)/b$ is the resolved stress and $\left(\vec{g}\times\vec{l}\right)/l$ is the unit vector normal to the dislocation line in the glide plane $(\vec{g}\perp\vec{l})$ (see Fig. 2). The force along the glide plane per unit length is then

$$f_{\sigma} = \left(\vec{g}\cdot\bar{\sigma}\cdot\vec{b}\right). \tag{7}$$

The surface of the layer systems considered in the present work may be assumed to be free of external forces, meaning that the stress is planar. In addition, while all the SiGe layer systems of interest here, (100), (110), (111), have at least orthorhombic symmetry so, it is useful to decompose the tensor $\bar{\sigma}$ in isotropic and tensile components normal to the layer: $\bar{\sigma} = \sigma(\bar{1} - \vec{n}\cdot\vec{n})$, where $\bar{\mathbf{1}}$ is a 3D unit matrix and $\vec{n}$ the unit normal vector on the layer. While the isotropic term does not contribute to the force along the glide plane, Eq. (7) becomes:

$$f_{\sigma} = (\vec{g}\cdot\vec{n})\cdot\left(\vec{b}\cdot\vec{n}\right) = Sb\sigma, \tag{8}$$

which holds for *any unit dislocation element in the glide plane*. The specific length scale is meaningful only for schematic straight dislocation model.

The factor S, called the Schmid factor, represents the force "strength"[30]

$$S = \left|(\vec{g}\cdot\vec{n})\cdot\left(\vec{b}\cdot\vec{n}\right)/b\right| = \cos\phi\cos\chi, \tag{9}$$

where the ϕ and χ are the angles between $\vec{g}$ and $\vec{n}$ and, $\vec{b}$ and $\vec{n}$, as indicated in the Fig. 2.

The above equation allows the determination of dislocations (their type) actively contributing to strain relaxation. A dislocation *does not* contribute to strain relaxation if the force acting on it along the glide plane is zero, $f_{\sigma} = 0$. This condition, translate to $S = 0$, and is fulfilled for following cases:

1. $\vec{b}$ is perpendicular to the layer plane, $\vec{b}\parallel\vec{n}$. Since $(\vec{g}\perp\vec{n})$ then $(\vec{g}\cdot\vec{n}) = 0$, (10a)
2. $\vec{b}$ is parallel to the layer plane, $\vec{b}\perp\vec{n}$. Then $(\vec{b}\cdot\vec{n}) = 0$. (10b)

Consequently, *a finite value of the relaxation active glide driving force*, f_{σ}, requires that the Burgers vector $\vec{b}$ *of the dislocation is oblique to the layer*. The Table III presents a simple exercise of the above discussion for the general case of straight dislocations in Si/Ge (FCC) system.

A useful application of the above considerations is the discussion of the active slip configurations for nucleation and propagation of dislocations contributing to strain relaxation for different layer symmetries. The glissile slip configuration in diamond cubic semiconductors, such as Si/Ge are $\{111\}\langle 110\rangle$ type. For a highly degenerated structure there are 24 distinct slip configurations possible (12 unique $\langle 110\rangle$ Burgers vectors and two $\{111\}$ glide planes per Brugers vector). The removal of the degeneracy by symmetry breaking in layer structures reduces the number the active slip configurations. For the pseudomorphic SiGe/Si(001) system, the symmetry reduces from cubic to tetragonal. Four $\{111\}$ glide planes allow generation and spreading of MDs, by SiGe shearing, in two $\langle 110\rangle$ directions. This results in a *biaxial relaxation* of SiGe layer.

In the case of pseudomorphic SiGe/Si(011) layers the symmetry reduces to orthorhombic. In contrast to the (100) surface orientation, two of the $\{111\}$ planes are

TABLE III. Line vectors, glide planes, dislocation type and their relevance for strain relaxation for Burgers vector $b = \langle 110\rangle/2$.

$\vec{b}$	[110]					
$\vec{l}$	[110]	$[1\bar{1}0]$	[101]	$[01\bar{1}]$	$[10\bar{1}]$	[011]
$\vec{g}$		(001)	$(1\bar{1}\bar{1})$		$(1\bar{1}1)$	
$\sphericalangle(\vec{b},\vec{l})$ (°)	0°	90°	60°			
(type)	screw	edge	mixed			
"relevant"	no		YES			

Downloaded 15 May 2013 to 134.94.122.141. This article is copyrighted as indicated in the abstract. Reuse of AIP content is subject to the terms at: http://jap.aip.org/about/rights_and_permissions

TABLE IV. The MDs, active glide planes as well as the active/inactive Burgers vectors for the (001) and (011) layer systems.

Surface					(**001**)								(**011**)			
MD-lines			[**110**]					[**1$\bar{1}$0**]					[**01$\bar{1}$**]			
Glide Planes	(**1$\bar{1}$1**)			(**1$\bar{1}\bar{1}$**)			(**111**)			(**11$\bar{1}$**)			(**111**)			(**1$\bar{1}\bar{1}$**)
Active BVs	[**011**]	[**10$\bar{1}$**]	[**01$\bar{1}$**]	[**101**]	[**01$\bar{1}$**]	[**10$\bar{1}$**]	[**011**]	[**101**]	[**10$\bar{1}$**]	[**10$\bar{1}$**]	[**110**]	[**0$\bar{1}\bar{1}$**]				
Inactive BVs					[**110**], [**1$\bar{1}$0**]								[**011**], [**01$\bar{1}$**]			

perpendicular to the layer plane ($\vec{\boldsymbol{g}} \perp \vec{\boldsymbol{n}}$) and the force on dislocations in these planes is zero. The restriction of shearing to the 2 active (111) and (1$\bar{1}$ $\bar{1}$) glide planes *oblique* to the SiGe layer results in a restriction in the formation of MDs to the [01$\bar{1}$] direction. This implies a *purely uniaxial relaxation* of the SiGe layer in the [100] direction. The MDs, active glide planes as well as the active/inactive Burgers vectors are listed in Table IV for the (001) and (011) layer systems. The straight forward calculation of the Schmid factor by applying Eq. (8) shows that *the force exerted on the dislocation is the same for both layer orientations*: $f_\sigma(001) = f_\sigma(011) = \sigma/\sqrt{6}$.

The above analytical discussions and results are in perfect agreement with the experimental results on the relaxation of SiGe/Si(001) and SiGe/Si(011) layers by He^+ or Si^+ ion implantation and annealing reported in the literature.[5,12,23,31] Yet, the absence of the relaxation for thin and low Ge content SiGe layers on (100) in contrast to the (011) system is not explained.

A. Anisotropy of the glide system

The symmetry of the layers and their associated dislocation dynamics alone, however, does not explain the difference in the relaxation efficiency of {100} and {110} SiGe layers of similar thickness, as observed experimentally.[12] This difference is attributed to the anisotropy of the dependence of the critical thickness for strain relaxation on the elastic strain in the layer, and will be discussed below.

The critical thickness above which the threading dislocations are able to move can be deduced from the balance of forces acting on every segment of the dislocation. The line tension $\boldsymbol{T}$ per unit length is given by[30]

$$f_T = \frac{\boldsymbol{T}}{w} = \frac{T}{h} = \sin\phi, \tag{11}$$

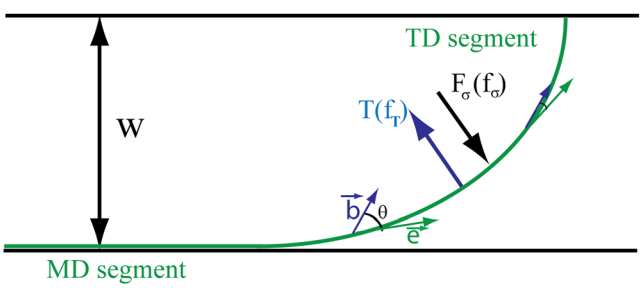

FIG. 3. (Color online) View on the glide plane indicating the forces on the dislocations and the evolution of θ.

where w is the width of the glide plane (where the $\boldsymbol{T}$ lies) and h is the layer thickness (see Fig. 3). From the force balance, using the Eqs. (8) and (9), the critical layer thickness for strain relaxation, h_c, under a stress, $\boldsymbol{\sigma_c}$, takes the form

$$h_c = \left(\frac{\sin\phi}{\cos\phi\cos\chi}\right)\frac{T}{b\boldsymbol{\sigma}_c} = \left(\frac{\tan\phi}{\cos\chi}\right)\frac{T}{b\boldsymbol{\sigma}_c}. \tag{12}$$

The term $\sin\phi$ is missing in the Matthews and Blakeslee theory[28] where the layer thickness h is inaccurately interpreted as dislocation length. Schwarz *et al.*[32] correctly used in their theoretical model of layer relaxation based on the dislocation—dislocation interaction a value "*ch*" for the thickness in the glide-plane and defined the constant "$c = \sqrt{3/2}$" as a constant relating the glide-plane thickness to the strained-layer thickness h. However, no general discussion or comment was made on the influence of the glide-plane width on the critical layer thickness or dislocation dynamics while only the specific case of the (001) Si system is treated.

The values of the term $A_g = (tg\phi/\cos\chi)$, which defines the *anisotropy of the glide system*, are listed in the Table V. From the Eq. (11) and Table V it can be concluded that *at given* ***stress*** *the critical thickness for strain relaxation is lowest/highest for (011)/(111) layer systems*, respectively. This explains the experimental results of the Ref. 12 and indicates that the 50 nm thick $Si_{0.85}Ge_{0.15}$ layer on (011) is "*supercritical*" but "*subcritical*" on (100) system orientation.

As derived above, dislocation glide is solely driven by the stress component transversal to the MD direction σ_t. For a quantitative treatment, this has to be related to the two principal axes (residual) strain component parallel, $\boldsymbol{\varepsilon_s}$, and transversal, $\boldsymbol{\varepsilon_t}$, to the MDs.

For the general case, $\boldsymbol{\varepsilon_t} \neq \boldsymbol{\varepsilon_s}$, the anisotropy plane stress/strain relation (Hooke's law), may be written as[33]

$$\sigma_t = \tilde{c}_{tt}\varepsilon_t + \tilde{c}_{ts}\varepsilon_s, \tag{13}$$

$$\sigma_t h_c = (\tilde{c}_{tt}\varepsilon_t + \tilde{c}_{ts}\varepsilon_s)h_c = \frac{A_g T}{b} \approx \mathbf{14}\,\boldsymbol{A_g}(\mathbf{Pa\,m}) \tag{14}$$

with $\tilde{c}_{tt} = c_{tt} - c_{nt}^2/c_{nn}$, and $\tilde{c}_{tt} = c_{ts} - c_{nt}c_{nt}/c_{nn}$ where $c_{tt}, \ldots$ are the elastic constant in the MD adapted coordinate system.

TABLE V. Calculated values for the anisotropy term A_g and $\langle\cos^2\theta\rangle$ for the main layer systems.

N	(001)	(011)	(111)
A_g	2	1.41	3.46
$\langle\cos^2\theta\rangle$	0.82	0.78	0.80

Downloaded 15 May 2013 to 134.94.122.141. This article is copyrighted as indicated in the abstract. Reuse of AIP content is subject to the terms at: http://jap.aip.org/about/rights_and_permissions

For the specific case of symmetric strain $\varepsilon_t = \varepsilon_s = \varepsilon$, it is preferable to express the h_c versus strain then stress. For elastic isotropic systems the MB relations are derived[28]

$$T = \frac{\mu b^2}{4\pi}\frac{1-\nu\langle\cos^2\theta\rangle}{1-\nu}\ln(\alpha w/b), \tag{15a}$$

$$\varepsilon h_c = \frac{A_g}{8\pi}\frac{\left(1-\nu\langle\cos^2\theta\rangle\right)}{1+\nu}\ln(\alpha w/b), \tag{15b}$$

where μ and ν are the shear modulus and the Poisson's ratio, α is the dislocation core parameter, w is the width of the glide plane, and $\langle\cos^2\theta\rangle$, with $\theta = \sphericalangle(\vec{b},\vec{e})$ where $\vec{e}$ is the unit vector along dislocation line, characterizes the dislocation character (edge, screw) and can be expressed by ϕ and χ. Using the curved dislocation model (as illustrated in Fig. 3), the values of $\langle\cos^2\theta\rangle = 1/2 + 2\cos\chi\sin\phi$, averaged along the dislocation (in the glide plane) gives a value of about 0.8, which reveals a close to "edge" dislocation character. In the following evaluations, we will use for all the layer systems $\langle\cos^2\theta\rangle \approx 0.8$ which introduces an acceptable error below 2%.

B. Critical conditions for layer relaxation

The first general condition for relaxation of a strained layer is that a threading dislocation (assume that is formed) is able to spread across the layer, creating and enlarging a strain relaxing MD at the SiGe/Si substrate interface. This process takes place if the layer thickness exceeds a critical thickness. However, this general requirement is completed by the following critical criteria: *The product of stress/strain and thickness,* as expressed by Eqs. (14) and (15b), *must be clearly larger than the critical value at the start and the end of relaxation.*

$$(\sigma,\varepsilon)h > \text{critical value}. \tag{16}$$

At the "start" because of the necessity of dislocation nucleation, at the "end" because of dislocation interactions and mutual blocking, associated with "work hardening," and because of the inhomogeneity of the MD distribution. Notice that neither dislocation nucleation nor mutual dislocation blocking or inhomogeneous MD distributions have been considered in deriving Eqs. (14) and (15). Consequently, increasing the efficiency of relaxation means minimizing these disturbing effects and reducing by this the product of stress/strain and thickness to low values close to the theoretical critical value given by Eq. (14). In order to evaluate the relaxation process a quality criteria can be introduced. The condition expressed by the Eq. (16) can be reformulated as: *the product of residual strain/stress and the layer thickness should be minimal,*

$$(\sigma,\varepsilon)_{res}h \sim \text{minimal}. \tag{17}$$

Accordingly, the ratio of the real (experiment) to ideal [Eq. (14)] critical thickness, defined as quality factor Q should be close to 1,

$$Q := \left(\tilde{c}_{tt}\varepsilon_t^{res} + \tilde{c}_{ts}\varepsilon_s^{res}\right)\frac{bh}{A_g T} \geq 1. \tag{18}$$

IV. COMPARISON OF THEORY AND EXPERIMENT

In order to prove the above model, we apply the above rationale to the experimental results we reported recently. Extensive studies were devoted to the development of innovative methods capable to introduce and drive, in a controlled way, threading dislocations required for strain relaxation.[5,34] Special attention was dedicated to ion implantation and annealing processes. The role of the implanted ions is to create planar defects, i.e., platelets or {311} defects for He or Si ion implantation, respectively, as sources for mobile loop formation and the relaxation process is then thermally driven. A thermal treatment alone, however, generates half loops at the top of the strained layer and by gliding toward the SiGe/Si substrate interface TDs pairs forms. This relaxation method results in a low degree of relaxation and for most of the cases, in a low crystalline quality of the relaxed layers.

For the following discussions, we have selected from our published data the layer parameters for which the ion implantation and annealing results in a "healthy" relaxation, meaning the highest degree of strain relaxation, and offer a high crystalline quality of the layers (low TDs density after relaxation).

Figure 4 shows the ideal relation between critical layer thickness versus the residual strain, according to Eq. 14, for partially relaxed $Si_{1-x}Ge_x$ layers in comparison to our experimental results recently published.

According to Eq. (15b) for a (001) layer where $A_g = 2$, for an ideal relaxation process a value of $\varepsilon h = \mathbf{0.15}$ is expected. The standard He^+ion implantation and annealing process offers only values in the range of 0.4 to 0.5. A relaxation closer to the ideal condition with a value of $\varepsilon h = 0.26$ was obtained for an improved layer structure by introducing a buried δ-Si:C layer in the Si(001) substrates.[27] This enhancement is attributed to localization, homogenization, and alignment of the He cavities along the δ-Si:C layer plane

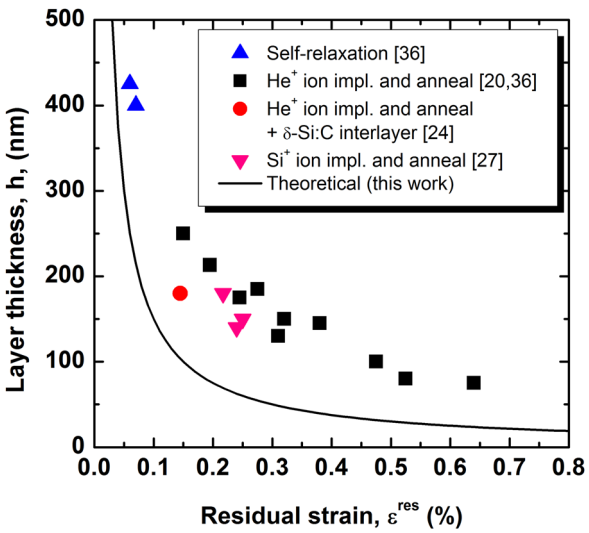

FIG. 4. (Color online) Layer thickness vs the residual strain. The solid line represents the theoretical model for the ideal critical thickness according to Eq. (14) while the symbols are our experimental data for SiGe(001) relaxation, published previously, for different relaxation methods, as indicated in the legend.

Downloaded 15 May 2013 to 134.94.122.141. This article is copyrighted as indicated in the abstract. Reuse of AIP content is subject to the terms at: http://jap.aip.org/about/rights_and_permissions

TABLE VI. Ratio of real to ideal critical thickness, Q, at the beginning and at the end of relaxation process, calculated for different implantation conditions and layer systems. The two rows for every layer system represent the initial (pseudomorph) and the final state (partially relaxed) of the SiGe layers.

Layer type	Ge content (%)	SiGe thickness (nm)	Relaxation degree (%)	Q	Ref.
SiGe/(100)Si	15	400	0	15	(43)
			87	2.2	
	15–30	75–250	0	≈9	(3), (23), (37)
	(23)	(180)	20–73	≈3.5	
			(70)		
	15	50	0	2.6	(12)
SiGe/Si/δ-Si:C on/(100)Si	23	180	0	11	(27)
			85	**1.7**	
SiGe/(110)Si	15	50	0 (on [100])	3.7	(12)
			10 (on [$\bar{1}$10])		
			62 (on [100])	2.0	
			10 (on [$\bar{1}$10])		
SiGe/(100)Si	20	180	0	9.3	(31)
			74	2.4	
	26	150	0	10	
			77	2.3	
	29	140	0	10.5	
			80	2.1	
1.4 μm [110]SiGe stripes on (011) Si	23	180	95 (on [$\bar{1}$10])	**0.9**	(37)
			45 (on [110])		
0.8 μm [110]SiGe stripes on (011) Si	23	180	95 (along [$\bar{1}$10])	**1.0**	(37)
			34 (along [110])		

improving the dislocation dynamics responsible for strain relaxation. A comparison of theory and experiment results is shown in Fig. 4 for strain relaxation of pseudomorphic SiGe layer grown on (001) Si. However, a more complete (general) discussion of the efficiency of the relaxation process can be made through the quality parameter Q. Table VI displays the ratio of real to ideal critical thickness, Q, at the beginning and the end of the relaxation process, for a broad range of experimental conditions and layer systems. For the conventional He^+ ion implantation on (001) samples, the relaxation efficiency increases with the layer thickness and with higher Ge content. For samples with comparable thicknesses, i.e., 180 nm and Ge content of 20 at. %, the Si^+ ion implantation enhances the strain relaxation efficiency, $Q = 2.4$, in respect to the conventional He^+ ion implantation method, $Q = 3.5$. The fundamental difference between the processes originates in the nucleation and evolution of the dislocation loops (TDs sources). In the He^+ ion implantation case, the high pressured gas filled cavities, formed during annealing, induce the formation of dislocation loops which are required to glide toward the SiGe/Si interface so that relaxation can occur. The inhomogeneous distribution of the dislocation loop sources may results in mutual blocking of gliding dislocation loops (reducing the density of the active loops). In contrast, for the Si^+ ion implantation method, the dislocation loops are directly formed in the SiGe layer by transformation from {311} planar defects.[35,36] The strain relaxation is constrained only by the formation of loops of a critical size and their extension through the SiGe layer to the surface and SiGe/Si substrate interface.[37] The localization and homogenization of dislocation loop sources for the He^+ ion implantation method, by introducing the δ-Si:C interlayer, the relaxation strongly increases, reducing the quality factor to 1.7, the closest to ideal experimental value for planar layer relaxation.

An excellent relaxation efficiency, $Q = 2$, was also obtained for (110)SiGe layer. In this case, the strain relaxation is pure uniaxial. The enhancement of the relaxation efficiency on (110) oriented surfaces is a direct consequence of the anisotropy of critical conditions for layer relaxation.

An interesting system is presented by the SiGe stripe relaxation.[37–39] The model suggests that the symmetry of the (001) relaxation can be reduced by patterning the SiGe layer into (sub) micrometer narrow [110] stripes. The average path length of TDs moving in the [$\bar{1}$10] direction is shortened by the two stripe boundaries, resulting in a reduction of the MD density in this direction and, correspondingly to a reduction of the degree of relaxation in the [110] direction. For stripes of 0.8 and 1.4 μm width an ideal factor $Q \sim 1$ is obtained. For this system, the analysis of XRD peak positions[40] yield *significantly lower* degrees of relaxation than ion channeling angular scans,[37] with a gap between both increasing with the asymmetry. In our comparison in the Table VI we have used the SiGe relaxation degree from Ref. 37 measured by ion channeling angular scans,[41] while x-ray diffraction has been shown to underestimate strain contributions of low MD densities and thus to overestimate the asymmetry in patterned structures.[42]

V. CONCLUSIONS

We have analytically analyzed and compared the plastic strain relaxation of SiGe layers for different layer orientation. For strain relaxation with He^+/H^+ ion implantation and

Downloaded 15 May 2013 to 134.94.122.141. This article is copyrighted as indicated in the abstract. Reuse of AIP content is subject to the terms at: http://jap.aip.org/about/rights_and_permissions

annealing gas filled platelets are less efficient in (011) than in (001) oriented layers as sources for misfit dislocations. The anisotropy of the resolved shear stress revealed as most important.

A flexible curved dislocation model is used to determine, the critical layer thickness versus strain/stress relation, given by two independent factors: the Schmid factor and the sinus of the angle between the active glide plane and the layer normal. Experimental data demonstrate that reduced values of the real-to-ideal ratio, close to 1, were obtained for improved layer relaxation by the introduction of δ-Si:C layers, by layer patterning and by the use of (011) layer orientation.

ACKNOWLEDGMENTS

This paper is dedicated to the memory of our colleague Dr. Helmut Trinkaus.

The authors thank Prof. K. Schröder (IFF, Forschngszentrum Juelich) for fruitful discussion.

[1]M. L. Lee, E. A. Fitzgerald, M. T. Bulsara, M. T. Currie, and A. Lochtefeld, J. Appl. Phys. **97**, 011101 (2005).
[2]R. Hull, J. C. Bean, J. M. Bonar, G. S. Higashi, K. T. Short, H. Temkin, and A. E. White, Appl. Phys. Lett. **56**, 2445 (1990).
[3]H. Trinkaus, B. Holländer, S. Rongen, S. Mantl, H.-J. Herzog, J. Kuchenbecker, and T. Hackbarth, Appl. Phys. Lett. **76**, 3552 (2000).
[4]K. Sawano, Y. Hirose, Y. Ozawa, S. Koh, J. Yamanaka, K. Nakagawa, T. Hattori, and Y. Shiraki, Jpn. J. Appl. Phys. **42**, 735 (2003).
[5]J. Cai, P. M. Mooney, S. H. Christiansen, H. Chen, J. O. Chu and A. J. Ott, J. Appl. Phys. **95**, 5347 (2004).
[6]B. Holländer, D. Buca, M. Mörschbächer, St. Lenk, S. Mantl, H.-J. Herzog, T. Hackbarth, R. Loo, M. Caymax, and P. F. P. Fichtner, J. Appl. Phys. **96**, 1745 (2004).
[7]G. Sun, Y. Sun, T. Nishida, and S. E. Thompson, J. Appl. Phys. **102**, 084501 (2007).
[8]S. F. Feste, T. Schäpers, D. Buca, Q. T. Zhao, J. Knoch, M. Bouhassoune, A. Schindlmayr, and S. Mantl, Appl. Phys. Lett. **95**, 182101 (2009).
[9]F. Lanzerath, D. Buca, H. Trinkaus, M. Goryll, S. Mantl, J. Knoch, U. Breuer, W. Skorupa, and B. Ghyselen, J. Appl. Phys. **104**, 044908 (2008).
[10]C. Ahn, N. Bennett, S. T. Dunham, and N. E. B. Cowern, Phys. Rev. B **79**, 073201 (2009).
[11]W. Heiermann, D. Buca, H. Trinkaus, B. Hollaender, U. Breuer, N. Kernevez, B. Ghyselen, and S. Mantl, ECS Transactions **19**, 95 (2009).
[12]R. A. Minamisawa, D. Buca, H. Trinkaus, B. Holländer, S. Mantl, V. Destefanis, and J. M. Hartmann, Appl. Phys. Lett. **95**, 034102 (2009).
[13]N. Hueging, M. Luysberg, K. Urban, D. Buca, and S. Mantl, Appl. Phys. Lett. **86**, 042112 (2005).
[14]K. Schwarz, Phys. Rev. Lett. **91**, 145503–1 (2003).
[15]H. Trinkaus, Radiation Effects and Defects in Solids **78**, 189 (1983).
[16]M. Hartmann and H. Trinkaus, Phys. Rev. Lett. **88**, 055505 (2002).
[17]J. Chen, P. Jung, and H. Trinkaus, Phys. Rev. Lett. **82**, 2709 (1999).
[18]P. F. P. Fichtner, J. R. Kaschny, A. Kling, H. Trinkaus, R. A. Yankov, A. Mücklich, W. Skorupa, F. C. Zawislak, L. Amaral, M. F. da Silva, and J. C. Soares, Nuclear Instruments and Methods in Physics Research B **136–138**, 460 (1998).
[19]L. D. Landau and E. M. Lifshitz, *Statistical Physics*, 3rd ed. (Butterworth-Heinemann, Oxford, 1996), Part 1.
[20]D. J. Eaglesham, A. E. White, L. C. Feldman, N. Moriya, and D. C. Jacobson, Rev. Lett. **70**, 1643 (1993).
[21]J. Chen, P. Jung, and H. Trinkaus, Phys. Rev. B **61**, 12923 (2000).
[22]N. Hueging, M. Luysberg, H. Trinkaus, K. Tillmann, and K. Urban, J. Mater Sci. **41**, 4454 (2006).
[23]D. Buca, B. Holländer, H. Trinkaus, S. Mantl, R. Carius, R. Loo, M. Caymax, and H. Schaefer, Appl. Phys. Lett. **85**, 2499 (2004).
[24]D. M. Isaacson, A. J. Pitera, and E. A. Fitzgerald, J. Appl. Phys. **101**, 013522 (2007).
[25]D. D'Angelo, S. Mirabella, E. Bruno, A. Terrasi, C. Bongiorno, F. Giannazzo, V. Raineri, G. Bisognin, and M. Berti, J. Appl. Phys. **103**, 016104 (2008).
[26]D. D'Angelo, S. Mirabella, E. Bruno, G. Pulvirenti, A. Terrasi, G. Bisognin, M. Berti, C. Bongiorno, and V. Raineri, J. Appl. Phys. **104**, 023501(2008).
[27]D. Buca, R. A. Minamisawa, H. Trinkaus, B. Holländer, N. D. Nguyen, R. Loo, and S. Mantl, Appl. Phys. Lett. **95**, 144103 (2009).
[28]J. W. Matthews and A. E. Blakeslee, J. Crystal Growth **27**, 118 (1974).
[29]J. P. Hirth and J. Lothe, *Theory of Dislocations*, 2nd ed. (Wiley, New York, 1982).
[30]D. Hull and D. J. Bacon, *Introduction to Dislocations* (Butterworth-Heinemann, 2001).
[31]D. Buca, R. A. Minamisawa, H. Trinkaus, B. Holländer, S. Mantl, R. Loo, and M. Caymax, J. Appl. Phys. **105**, 114905 (2009).
[32]K. W. Schwarz and Y. Tu, J. Appl. Phys. **106**, 083510 (2009).
[33]C. Hwu, *Anisotropic Elastic Plates* (Springer, New York, 2010), ISBN 978-1-4419-59-14-0.
[34]Y. Hoshi, K. Sawano, A. Yamada, N. Usami, K. Arimoto, K. Nakagawa, and Y. Shiraki, J. Appl. Phys. **107**, 103509 (2010).
[35]B. Colombeau, N. E. Cowen, F. Cristiano, P. Calvo, N. Cherkashin, Y. Lamrani, and A. Claverie, Appl. Phys. Lett. **83**, 1953 (2003).
[36]F. Cristiano, J. Grisolia, B. Colombeau, M. Omri, B. de Mauduit, A. Claverie, L. F. Giles, and N. E. B. Cowern, J. Appl. Phys. **87**, 8420 (2000).
[37]D. Buca, B. Holländer, S. Feste, S. Lenk, H. Trinkaus, S. Mantl, R. Loo, and M. Caymax, Appl. Phys. Lett. **90**, 032108 (2007).
[38]H. Yin, R. L. Peterson, K. D. Hobart, S. R. Shieh, T. S. Duffy, and J. C. Sturm, Appl. Phys. Lett. **87**, 061922 (2005).
[39]R. Z. Lei, W. Tsai, I. Aberg, T. B. O'Reilly, J. L. Hoyt, D. A. Antoniadis, H. I. Smith, A. J. Paul, M. L. Green, J. Li, and R. Hull, Appl. Phys. Lett. **87**, 251926 (2005).
[40]A. Rehman Khan, J. Stangl, G. Bauer, D. Buca, B. Holländer, H. Trinkaus, S. Mantl, R. Loo, and M. Caymax, Semicond. Sci. Technol. **22**, S212 (2007).
[41]H. Trinkaus, D. Buca, B. Holländer, R. A. Minamisawa, S. Mantl, and J. M. Hartmann, J. Appl. Phys. **107**, 124906 (2010).
[42]H. Trinkaus, D. Buca, B. Holländer, S. Mantl, A. R. Khan, and G. Bauer, Conference Digest of the Third International Silicon Germanium Technology and Devices Meeting (IEEE, New York, 2006), p. 120, 15–17 May.
[43]D. Buca, J. Morschbacher, B. Holländer, M. Luysberg, R. Loo, M. Caymax, and S. Mantl, Material Research Society Symposium Proceeding **809**, 15 (2004).

Downloaded 15 May 2013 to 134.94.122.141. This article is copyrighted as indicated in the abstract. Reuse of AIP content is subject to the terms at: http://jap.aip.org/about/rights_and_permissions